

Anomalous optical phonons in FeTe chalcogenides: Spin state, magnetic order, and lattice anharmonicity

V. Gnezdilov,¹ Yu. Pashkevich,² P. Lemmens,³ A. Gusev,² K. Lamonova,² T. Shevtsova,² I. Vitebskiy,⁴ O. Afanasiev,¹ S. Gnatchenko,¹ V. Tsurkan,^{5,6} J. Deisenhofer,⁵ and A. Loidl⁵

¹*B. I. Verkin Institute for Low Temperature Physics and Engineering of the National Academy of Sciences of Ukraine 47 Lenin Ave., Kharkov 61103, Ukraine*

²*A. A. Galkin Donetsk Phystech of the National Academy of Sciences of Ukraine, Donetsk 83114, Ukraine*

³*Institute for Condensed Matter Physics, TU Braunschweig, D-38106 Braunschweig, Germany*

⁴*University of California at Irvine, Irvine, CA 92697, USA*

⁵*Experimental Physics V, University Augsburg, 86159 Augsburg, Germany*

⁶*Institute of Applied Physics, Academy of Sciences of Moldova, MD-2028 Chisinau, R. Moldova*

(Received 1 February 2011; revised manuscript received 26 April 2011; published 27 June 2011)

Polarized Raman-scattering spectra of nonsuperconducting, single-crystalline FeTe are investigated as a function of temperature. We have found a relation between the magnitude of ordered magnetic moments and the linewidth of A_{1g} phonons at low temperatures. This relation is attributed to the intermediate spin state ($S = 1$) and the orbital degeneracy of Fe ions. Spin-phonon coupling constants have been estimated based on microscopic modeling using density functional theory and analysis of the local spin density. Our observations show the importance of orbital degrees of freedom for Fe-based superconductors with large ordered magnetic moments, while the small magnetic moment of Fe ions in some iron pnictides reflects the low spin state of Fe ions in those systems.

DOI: [10.1103/PhysRevB.83.245127](https://doi.org/10.1103/PhysRevB.83.245127)

PACS number(s): 74.70.Xa, 74.25.Kc

I. INTRODUCTION

The report of superconductivity at 26 K in iron pnictides¹ and iron chalcogenides² has triggered an intense burst of research activity comparable to that during the early days after the discovery of superconducting cuprates or hydrated cobaltates $\text{Na}_x\text{CoO}_2 \cdot y\text{H}_2\text{O}$. The search for new superconducting materials and attempts to raise superconducting transition temperatures T_c by chemical doping³⁻⁶ and by external pressure⁷⁻¹⁰ have led to the discovery of other members of iron pnictide and chalcogenide families with higher T_c . The presence of a layered crystal structure with Fe ions in tetrahedral coordination is a general structural feature of iron-based compounds. This main building block possesses a tetragonal planar symmetry at room temperature, which is associated with certain degeneracy of electronic and phononic spectra. Simultaneously, many theoretical scenarios were evaluated. However, not only the superconductivity mechanism, but also the magnetic properties of iron-based compounds remain disputable. All scenarios agree with respect to the crucial importance of the distance between the Fe surrounding ligands and the Fe plane on the electronic ground state. Raman scattering on phonons that modulate these distances could shed light upon the interplay between lattice, charge, orbital, spin degrees of freedom, and superconductivity.

The chalcogenide family $\text{Fe}_{1+y}\text{Se}_x\text{Te}_{1-x}$ occupies a special place among newly discovered iron superconductors. Firstly, the members of this family have very simple stoichiometry, while their crystal structure can be seen as a stack of $\text{FeSe}_x\text{Te}_{1-x}$ layers. Secondly, Fe_{1+y}Te has an unusual magnetic translation symmetry with an in-plane magnetic propagation vector $k_1 = (\pi/a, 0)$, rather than $k_0 = (\pi/a, \pi/a)$ observed in ReFeAsO .¹¹ This kind of magnetic ordering is associated with the rare phenomenon of (orthorhombic) magnetostriction of purely exchange nature. Finally, the most remarkable feature of $\text{Fe}_{1+y}\text{Se}_x\text{Te}_{1-x}$ is its large magnetic

moment, which is the highest among the pnictides, reaching $2.5 \mu_B/\text{Fe}$ for $\text{Fe}_{1.05}\text{Te}$.¹² By comparison, the maximum moment for 1111 materials does not exceed $0.4 \mu_B/\text{Fe}$, and it does not exceed $1 \mu_B/\text{Fe}$ for 122 materials.¹³ The fact that the intermediate spin state ($S = 1$) of Fe ions is realized in FeTe implies that the orbital degrees of freedom of Fe ions play an important role in this compound.^{14,15}

In this paper, we present the results of theoretical and experimental study of phonon Raman scattering in non-superconducting Fe_{1+x}Te . Zone-centered and Raman-active phonons are classified by the irreducible representations of the space symmetry group of the crystal. First-principles lattice-dynamics calculations are performed for the monoclinic magnetic phase of FeTe. Our theoretical and experimental results appear to be in good agreement. The remarkable temperature dependence of the phonon modes in FeTe is discussed in the context of its electronic properties.

II. EXPERIMENT

Single crystals of $\text{Fe}_{1.051}\text{Te}$ were grown using Bridgman and self-flux methods. The actual composition was determined by x-ray analysis as $\text{Fe}_{1.051}\text{Te}$ [with $a = 3.8220(1) \text{ \AA}$ and $c = 6.2889(1) \text{ \AA}$]. A drastic drop in $\chi(T)$ observed at $T_N \approx 70 \text{ K}$ is attributed to antiferromagnetic ordering. Raman scattering experiments were carried out in quasibackscattering geometry. A solid-state laser was used for an excitation at 532.1 nm. To protect the sample from heating, the laser output power was kept below 5 mW on a focus of approximately 50 μm diameter. The spectra were measured in two polarization configurations (parallel XX and crossed XY) within the crystallographic ab plane. The scattered light was collected and dispersed by a triple monochromator DILOR XY on a liquid-nitrogen-cooled CCD detector. The measurements were taken in a variable temperature closed-cycle cryostat (Oxford/Cryomech Optistat, $T = 2.8\text{--}300 \text{ K}$).

III. RESULTS AND DISCUSSION

At room temperature, the single-phase FeTe(Se) has the tetragonal PbO structure (space group $P4/nmm$).^{2,16–18} In this phase, iron chalcogenide forms the same edge-sharing antiferrofluorite layers also found in FeAs superconductors. Fe and Te ions occupy 2a and 2c Wyckoff positions, respectively. Symmetry analysis shows that there are four Raman-active modes [$A_{1g}(\text{Te}) + B_{1g}(\text{Fe}) + 2E_g(\text{Te, Fe})$] and two infrared-active modes [$A_{2u}(\text{Te, Fe}) + E_u(\text{Te, Fe})$]. The Raman tensors take the form:

$$A_{1g} = \begin{pmatrix} a & 0 & 0 \\ 0 & a & 0 \\ 0 & 0 & b \end{pmatrix}, \quad B_{1g} = \begin{pmatrix} c & 0 & 0 \\ 0 & -c & 0 \\ 0 & 0 & 0 \end{pmatrix},$$

$$\text{and } E_g = \begin{pmatrix} 0 & 0 & -e \\ 0 & 0 & e \\ -e & e & 0 \end{pmatrix}.$$

At $T_s = 70$ K, metallic FeTe undergoes a first-order phase transition from tetragonal to monoclinic phase, and below 70 K, its space symmetry group is $P2_1/m$.^{12,19,20} This phase transition is accompanied by u_{xz} -type distortion and simultaneous antiferromagnetic ordering. Noticeably, the symmetry of the long-range magnetic order below 70 K is such that it is compatible with the observed monoclinic structural distortion accompanying the phase transition. This suggests that, at least from a symmetry point of view, crystal distortions below 70 K could be a result of the antiferromagnetic ordering, similar to the phenomenon of magnetostriction. If this is the case, the phase transition at 70 K is magnetic in nature, while the crystal distortions are a secondary effect. A way to prove or disprove this assumption is to destroy the antiferromagnetic order by applying a sufficiently strong magnetic field and see if the structural distortions persist. Since we did not conduct such measurements, we cannot speculate on the physical nature of the phase transition.

In addition to a change in the lengths of the a and b axes, the length of the c axis increases by nearly 0.02 \AA , and its direction rotates towards the a axis, creating a slightly acute angle $\beta = 89.2^\circ$. As a result, the only remaining twofold symmetry axis is the b axis.^{12,19} The u_{xz} distortion leads to a change in the x and z coordinates for both Fe and Te atoms and to a small corrugation of the Fe plane. In this case, all atoms occupy the same 2e Wyckoff positions, each of which contributes to three Raman active modes ($2A_g + B_g$). Raman tensors take the form:

$$A_g = \begin{pmatrix} a & d & 0 \\ d & b & 0 \\ 0 & 0 & c \end{pmatrix} \quad \text{and} \quad B_g = \begin{pmatrix} 0 & 0 & e \\ 0 & 0 & f \\ e & f & 0 \end{pmatrix}.$$

The two different 1D representations A_{1g} and B_{1g} of the tetragonal symmetry group correspond to the same 1D representation A_g of the monoclinic symmetry group, while the double degenerate irreducible representation E_g splits into A_g and B_g . The latter could lead to some leakage of previous E_g modes to our geometry of Raman spectra

measurements at low temperatures. Note that the extra Fe ions in Fe_{1+y}Te occupy the same 2c positions as the Te ions in the tetragonal phase and 2e position in the monoclinic phase.^{12,19}

The zone-center phonons and the electronic structure of the FeTe in the monoclinic magnetic phase have been calculated within the framework of density functional theory (DFT). We applied the all-electron full-potential linearized augmented plane wave method (Elk code)²¹ with the local spin density approximation (LSDA)²² for the exchange-correlation potential and with the revised generalized gradient approximation of Perdew–Burke–Ernzerhof (PBEsol).²³ We used the experimental unit cell parameters from $\text{Fe}_{1.05}\text{Te}$ at 2 K¹² with structure optimization and with the unit cell lattice constants fixed. In our theoretical calculations, the magnitude of the iron magnetic moments was chosen to provide the best agreement between theoretical and experimental phononic spectra. The magnetic unit cell in our model is composed of two crystallographic monoclinic unit cells related by the primitive translation along the a axis. For simplicity, we assume in our computations that the magnetic moments of iron are parallel to the c axis with the same antiferromagnetic sign alternation as that of the real magnetic structure.¹² We did not account for unit cell doubling along the c axis. Our analysis shows a strong dependence of the phonon frequencies on the magnitude of iron magnetic moments and on the tellurium height (z coordinate).

Figure 1 shows the polarized Raman spectra of single crystal $\text{Fe}_{1.05}\text{Te}$ at $T = 290$ and 20 K in XX and XY scattering configurations. Two strong lines can be easily identified in the spectra. At room temperature, these lines are located

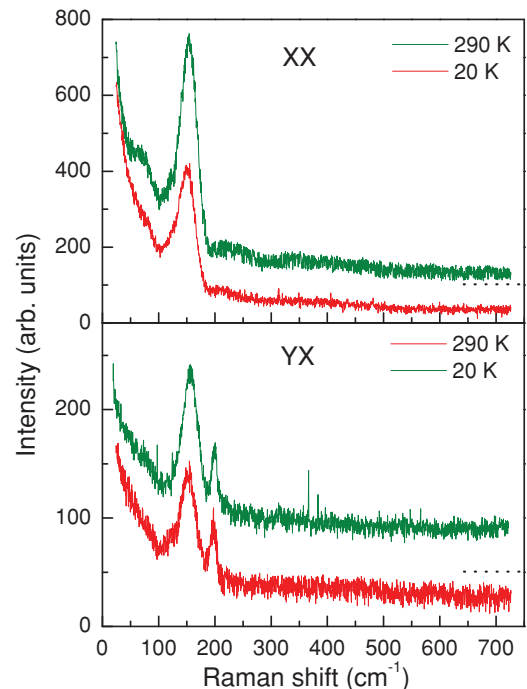


FIG. 1. (Color online) Raman spectra of single crystal $\text{Fe}_{1.05}\text{Te}$ taken in quasibackscattering from the ab plane at two temperatures. For clarity, the green curves are shifted in the vertical direction as indicated.

TABLE I. The results of phonon-mode calculations and a comparison with data from Raman experiments.

Symmetry ($P4/nmm$)	Symmetry ($P2_1/m$)	Atoms and its displacements	Frequencies (cm^{-1})	
			Theory ($P2_1/m$) Γ - point $k = 0$	Experimental data (80 K)
E_g	B_g	(Fe + Te, $u_{x+/-y}$)	76.8	
E_g	A_g		86.8	
A_{1g}	A_g	(Te, $u_{1z} - u_{2z}$)	164.5	155.2
E_u	A_u		173.5	
E_u	B_u	(Fe + Te)	195.7	
B_{1g}	A_g	(Fe, $u_{1z} - u_{2z}$)	206.5	201.4
E_g	B_g	(Fe + Te, $u_{x+/-y}$)	214.8	
E_g	A_g		243.6	
A_{2u}	A_u	(Fe, $u_{1z} + u_{2z}$)	256.2	

at 151 and 197 cm^{-1} and were earlier assigned to $A_{1g}(\text{Te})$ and $B_{1g}(\text{Fe})$ phonon modes, respectively.^{24–26} In Table I, we compare our experimental results with numerical simulations. The comparison shows a very good agreement between our theoretical and experimental phononic spectra, provided that we set the iron magnetic moment to be equal to 2.5 μ_B . Surprisingly, this value turns out to be very close to the experimental value 2.52 μ_B of the iron magnetic moment.¹² Also the tellurium height we obtained, $z_{\text{theo}} = 0.276$, is in nice agreement with the experimental one, $z_{\text{exp}} = 0.28$.¹² This suggests that for FeTe the above feature is in accordance with Yildirim's finding for Fe-As 1111 and 122 compounds.²⁷

Indeed, the latter study also shows a strong relation of the phonon spectra with the magnetic moment of Fe sublattices. Importantly, phonon frequencies obtained in our numerical computations are in much better agreement with experiments than those obtained in earlier modeling.^{24–26} The reason for that is, in the computations conducted in Refs. 24–26, the magnitude of the iron magnetic moment has not been taken into account explicitly. In our analysis, we did not account for the contribution from the excess iron; although, in accordance with the scenario developed in Ref. 28, even a small Fe excess strongly changes the FeTe Fermi surface toward a nesting condition along $(\pi/a, 0)$.

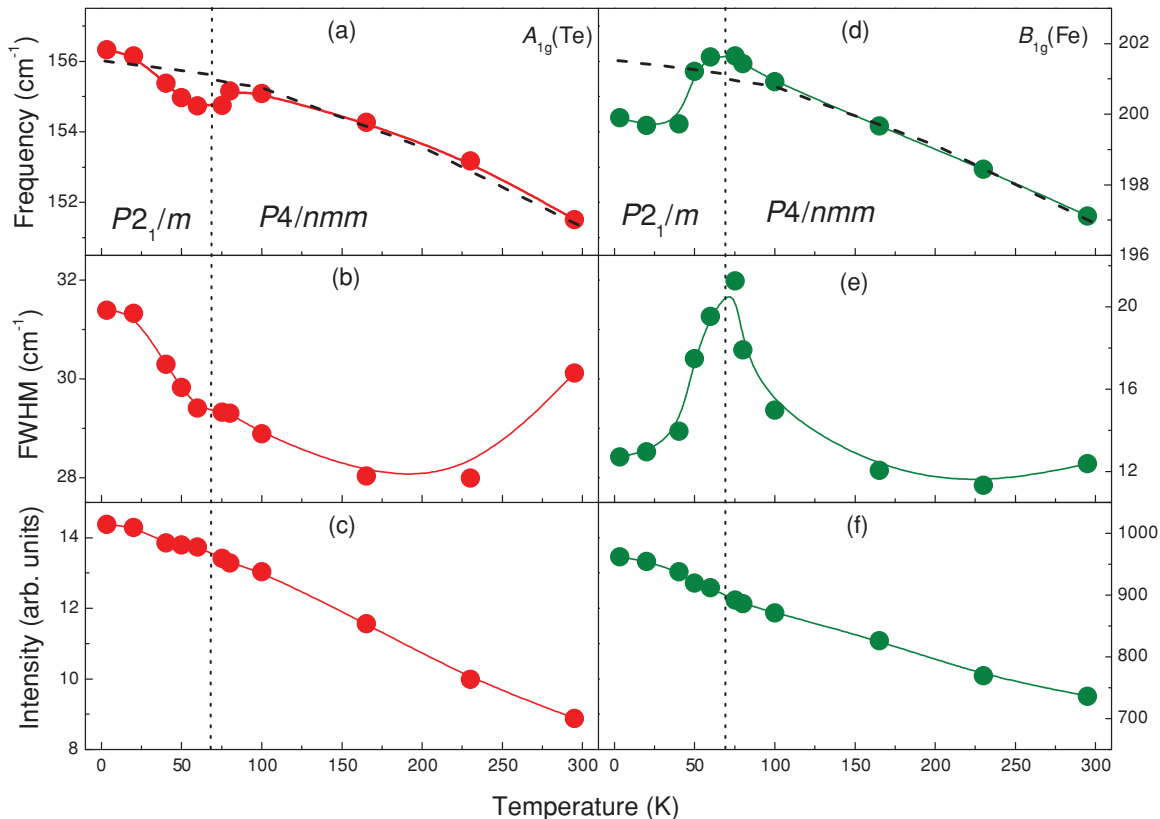


FIG. 2. (Color online) Parameters of two phonon modes in $\text{Fe}_{1.051}\text{Te}$. (a) and (d) Temperature dependence of the frequency (solid circles) together with the fit using Eq. (1) (dashed lines). (b) and (e) Linewidth, FWHM. (c) and (f) Integrated intensity. Solid lines in (b), (c), (e), and (f) are a guide to the eyes.

In Fig. 2, we show the temperature-dependent parameters of the A_{1g} and B_{1g} phonon modes. The T dependencies of the frequencies of both A_{1g} and B_{1g} modes show anomalies in the region of the structural transition and magnetic ordering temperature. Using data from Ref. 12 for the temperature change of the lattice constants of $\text{Fe}_{1.05}\text{Te}$, we fit the frequency temperature dependencies with Grüneisen's law:

$$\frac{\Delta\omega_i(T)}{\omega_i(290)} = -\gamma_i \frac{\Delta V_0(T)}{V_0(290)} \quad (1)$$

Here V_0 is the primitive cell volume, and all differences are calculated from values at ambient temperature. In the tetragonal phase, the Grüneisen parameters equal $\gamma_{B_{1g}}(\text{Fe}) = 2.15$ and $\gamma_{A_{1g}}(\text{Te}) = 2.85$, both of which deviate from the usual value $\gamma \approx 2$. The larger deviation for the Te mode evidences a stronger impact of anharmonicity, which is expected from the position of this atom in the lattice. At the same time, the change of the primitive cell volume V_0 in the monoclinic phase demonstrates a rather smooth dependence (Fig. 11 in Ref. 12). Thus, we conclude that the frequency deviation of a phonon from smoothly varying behavior versus T may be associated with the onset of magnetic ordering.

The renormalization of the phonon frequency below the magnetic ordering temperature is caused by a phonon modulation of the magnetic interactions, which includes superexchange, direct exchange (in metal), and anisotropy.²⁹ Spin-phonon coupling H_{sp} presents a quadratic form of the magnetic and the mediated ligand ion's displacements. Supposing that the main contribution to spin-phonon coupling results from the Fe-Te-Fe bond-angle modulation of the exchange interactions, we obtain:

$$H_{sp} = [\lambda_{nnn}^{(I)} (Q_{\text{Fe}}^2 + Q_{\text{Te}}^2) + \lambda_{nnn}^{(II)} Q_{\text{Fe}} Q_{\text{Te}} + \lambda_{nn} (Q_{\text{Te}}^2 - Q_{\text{Fe}}^2)] L_1^2(k_I) \quad (2)$$

Here, $Q_{\text{Fe}} = u_{1z}(\text{Fe}) - u_{2z}(\text{Fe})$ and $Q_{\text{Te}} = u_{1z}(\text{Te}) - u_{2z}(\text{Te})$ are symmetry adapted modes of atom displacements along the z axis for $B_{1g}(\text{Fe})$ and $A_{1g}(\text{Te})$ phonons, respectively. Atom enumeration and the magnetic structure are shown in Fig. 3. $L_1(k_I) = S_1(k_I) + S_2(k_I)$ is the magnetic order parameter constructed from Fourier components of the α sublattice's magnetic moments $S_\alpha(k_I)$. The first and the second term in H_{sp} originate from modulations of the next nearest neighbors (nnn) interaction J_{2a} and J_{2b} (hereafter, we use the notation of Ref. 28). The third term comes from the modulation of the nearest neighbor (nn) J_{1a} and J_{ab} interactions.

In spite of their exchange origin, the spin-phonon coupling constants $\lambda_{nn/nnn}$ are rather small due to their proportionality to the magnitude of monoclinic distortion u_{xz} , which is induced by the first-order structural phase transitions $P4/nmm \rightarrow P2_1/m$. Using this smallness, one can derive a magnetically induced frequency shift of ω_{Fe} and ω_{Te} phonon frequencies taken at 80 K slightly above T_N :

$$\begin{aligned} \Delta\omega_{\text{Fe/Te}} &= \frac{1}{2\omega_{\text{Fe/Te}}} \left\{ \frac{\lambda_{nnn}^{(I)} - / + \lambda_{nn}}{m_{\text{Fe/Te}}} + / - \frac{\lambda_{nnn}^{(II)2}}{(\omega_{\text{Fe}}^2 - \omega_{\text{Te}}^2)m_{\text{Fe}}m_{\text{Te}}} \right\} \\ &\times L_1^2(k_I). \end{aligned} \quad (3)$$

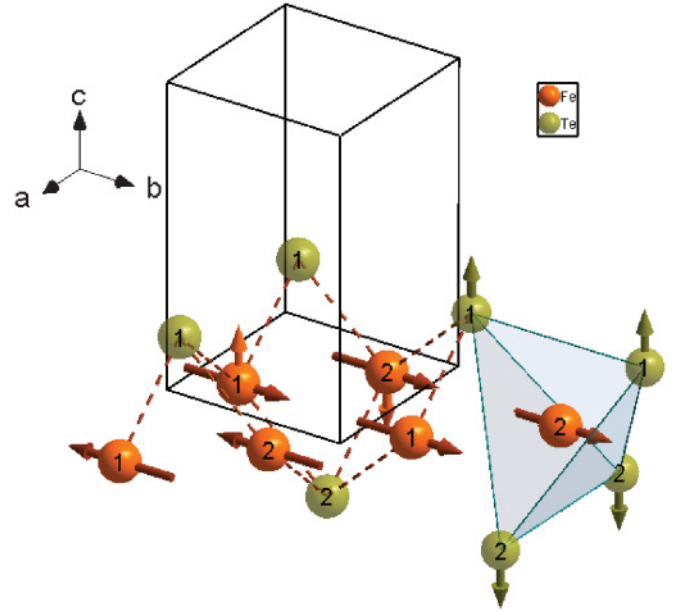


FIG. 3. (Color online) Magnetic structure of FeTe in the monoclinic phase $P2_1/m$ with the magnetic propagation vector $k_I = (\pi/a, 0)$. Magnetic moments are shown by dark arrows drawn through the atoms. $A_{1g}(\text{Te})$ and $B_{1g}(\text{Fe})$ ions' displacements are shown by arrows drawn from the ions.

where $m_{\text{Fe/Te}}$ are atomic masses. From Eq. (3) we obtain a renormalization of the phonon frequency in magnetic compounds^{30,31} $\omega_{ph} = \omega_{0ph} + \lambda_{ph}\eta^2$, which traces the temperature dependence of the square of a magnetic order parameter $\eta(T)$. The coupling coefficient λ_{ph} is different for each phonon and may have either sign. In our case, one can neglect contribution from $\lambda_{nnn}^{(II)}$, which always leads to a repulsion of phonon frequencies, due to its second-order smallness. Contributions from the $\lambda_{nnn}^{(I)}$ term change the phonon frequencies in identical ways, either positive or negative, while the contribution from the λ_{nn} term changes the phonon frequencies in the opposite way.

As follows from data shown in Figs. 2(a) and 2(d), at lowest temperature (3 K), the shift of the former $B_{1g}(\text{Fe})$ phonon mode is negative, while for the former $A_{1g}(\text{Te})$ phonon mode, it is positive. Taking into account both these shifts calculated relative to fitting curves, at 3 K, we estimated the spin-phonon coupling constants, which are $\lambda_{nn} = 3.6(9) \cdot 10^{-6} \text{ meV}/(\text{\AA} \mu_B)^2$ and $\lambda_{nnn}^{(I)} = -1.9(5) \cdot 10^{-6} \text{ meV}/(\text{\AA} \mu_B)^2$. Here we chose $L_{1y}(k_I) = 5.08 \mu_B$ in accordance with data from Ref. 12.

There is another nontrivial contribution to the phonon frequency renormalization which is specific to the magnetic phase in iron pnictides and chalcogenides. Unlike in the case of regular magnetic materials, the antiphase motion of chalcogens (or pnictogens) surrounding Fe ions not only modulates the exchange interactions, but also affects the magnitude of the iron magnetic moment. Here we refer to a recent paper by C. V. Moon and H. J. Choi,³² where it is stressed that the ordered magnetic moment in FeTe depends on the value of the tellurium z coordinate. This mechanism cannot be reduced to the form given in Eqs. (2) or (3), and at lowest temperatures, its contribution should be negligible, since the magnetic moment becomes temperature independent. Also this

mechanism should not be relevant to the Fe B_{1g} vibration, as it modulates the Fe-Te distances in an opposite way, making them shorter-longer, simultaneously. We therefore relate the unusual frequency shift of the $A_g(\text{Te})$ mode in the magnetically ordered phase to contributions of this mechanism.

A very unexpected behavior of the A_{1g} and B_{1g} phonon linewidth [Figs. 2(b) and 2(e)] is observed in our experiments on $\text{Fe}_{1.051}\text{Te}$ single crystals. In addition to the anomalies at T_s , the full width at half maximum (FWHM) increases pronouncedly on cooling below approximately 150 K. Interestingly, as was found in neutron powder diffraction experiments,³³ the FWHM of the (200) peak increases on cooling below the same temperature for all the specimens of $\text{FeSe}_{1-x}\text{Te}_x$. However, the last observation was interpreted as a decrease in the symmetry of the high-temperature tetragonal structure at around $T = 150$ K, even if the (200) peak does not split. The most puzzling feature we observe is in the monoclinic phase, where the FWHM of $A_g(\text{Te})$ mode increases, while the width of the $A_g(\text{Fe})$ modes decreases and returns back to the value it had in the tetragonal phase.

In the following, we will discuss the relation of the Fe magnetic moment and anharmonicity. Solely chalcogen's (pnictogen's) antiphase vibrations that occur perpendicular to the Fe layer have an internal source of anharmonicity. Indeed, as one can see from Fig. 3, the A_{1g} type of Te vibrations play the role of a breathing-like mode for the chalcogen's (pnictogen's) tetrahedra. In a localized-electron framework, some modulation of Fe-Te distances (i.e. radii of $\text{Fe}^{2+}-3d^6$ ion) can induce a spin state instability of Fe^{2+} at which the intermediate spin state ($S = 1$) possesses a larger ionic radius, and the low spin state ($S = 0$) corresponds to a smaller one (see, for instance, Refs. 34 and 35). Such a modulation is specific for an intermediate spin state, i.e. for the Fe spin state with highest magnetic moment, because of its direct connection with an orbital reorder. Furthermore, a few ground-state orbital ordering patterns, which are consistent with the magnetically ordered structure, have been addressed in iron pnictide superconductors.¹⁵ Thus spin-orbital frustration accompanied with magnetic order with large Fe magnetic moments is associated with anharmonicity. Interestingly, as shown recently for FeO molecules,³⁶ variations of the metal-ligand distances lead not only to a redistribution of the spin density, but also to a modification of the adiabatic potential. Again, the B_{1g} vibration of Fe ions should not be affected by this mechanism due to the Fe layer topology. We arrive at the conclusion that orbital degrees of freedom in general, and particularly spin-orbital frustrations, are responsible for the anomalous increase in width of the $A_g(\text{Te})$ mode in the FeTe compound. Note that the fundamental role of the orbital degrees of freedom in the formation of electronic and magnetic excitations in $\text{FeSe}_{0.5}\text{Te}_{0.5}$ has been proven based on recent inelastic neutron studies.³⁷

By accepting these arguments, one should check cases where this mechanism is not applicable, i.e. for the low-value magnetic moment when the Fe^{2+} is close to low spin state and orbital degrees of freedom become irrelevant. Indeed, a close inspection of available Raman data on $A_{1g}(\text{As})$ phonons in undoped 1111 compounds³⁸ and 122 compounds,^{39,40} all of which possess a low value of magnetic moment,¹³ demonstrates that in the magnetically ordered state the width of this phonon mode always decreases under temperature lowering. This is in accordance with our expectation. One can also deduce that orbital fluctuations in 1111 and 122 materials, if they exist in paramagnetic phase, become suppressed in the magnetically ordered state.

The relevance of other mechanisms of electron-phonon coupling to the discussed phonons should be excluded by the following reason. There exists a remarkable resistivity drop in the magnetically ordered phase for both FeTe ¹¹ and SrFe_2As_2 ,⁴⁰ while the width of $A_{1g}(\text{Te}/\text{As})$ modes demonstrates the opposite change with temperature. The only difference between the magnetic states of the FeAs/Te layers is the magnitude of iron magnetic moments that point to the different involved orbital states.

The intensity data for the two phonons given in Figs. 2(c) and 2(f) exhibit an increase with decreasing temperature and do not show any anomaly within our experimental resolution.

We would like to highlight that we ascribe the giant splitting of originally degenerate E_g modes in the monoclinic magnetic phase (see Table I) to spin-lattice interaction of purely exchange (Coulomb) nature. The cases of symmetry reducing spin-lattice interaction of exchange nature are extremely rare. They can be very important because the respective distortion can be much stronger compared to the regular case of relativistic spin-lattice interaction. Note that a large splitting of E_g modes has been observed in BaFe_2As_2 .⁴¹ Recall that normally lattice distortions in magnetic materials are associated with relativistic spin-lattice interactions, which are usually much weaker.

To summarize all above arguments, we stress that the A_{1g} (chalcogen/pnictogen) phonon linewidth is a marker of the actual Fe orbital state in the parent compounds of iron-based superconductors. Orbital degrees of freedom should be taken into account in systems with large magnetic moments.

ACKNOWLEDGMENTS

This work was supported by Russian-Ukrainian Grant No. 9-2010 and FRFSF of Ukraine Grant No. F29.1/014 and the German Science Foundation via DFG LE 967/6-1, SPP 1458 and TRR 80. The calculations have been performed at the grid cluster of Donetsk PhysTech NASU under support of Grant N232. Yu.P. acknowledges partial support from the Swiss National Science Foundation (Grant SNSF IZKOZ2.134161).

¹Y. Kamihara, T. Watanabe, M. Hirano, and H. Hosono, *J. Am. Chem. Soc.* **130**, 3296 (2008).

²F. C. Hsu, J. Y. Luo, K. W. Yeh, T. K. Chen, T. W. Huang, P. M. Wu, Y. C. Lee, Y. L. Huang, Y. Y. Chu, D. C. Yan, and M. K. Wu, *Proc. Natl. Acad. Sci. USA* **105**, 14262 (2008).

³M. Rotter, M. Tegel, and D. Johrendt, *Phys. Rev. Lett.* **101**, 107006 (2008).

⁴J. H. Tapp, Z. Tang, B. Lv, K. Sasmal, B. Lorenz, P. C. W. Chu, and A. M. Guloy, *Phys. Rev. B* **78**, 060505(R) (2008).

- ⁵X. H. Chen, G. W. T. Wu, R. H. Liu, and D. F. Fang, *Nature (London)* **453**, 761 (2008).
- ⁶Z. A. Ren, J. Yang, W. Lu, W. Yi, X. L. Shen, Z. C. Li, G. C. Che, X. L. Dong, L. L. Sun, F. Zhou, and Z. X. Zhao, *Chin. Phys. Lett.* **25**, 2215 (2008).
- ⁷H. Takahashi, *Nature (London)* **453**, 376 (2008).
- ⁸M. S. Torikachvili, S. L. Bud'ko, N. Ni, and P. C. Canfield, *Phys. Rev. Lett.* **101**, 057006 (2008).
- ⁹Y. Mizuguchi, F. Tomioka, Sh. Tsuda, T. Yamaguchi, and Y. Takano, *Appl. Phys. Lett.* **93**, 152505 (2008).
- ¹⁰S. Medvedev, T. McQueen, I. A. Troyan, T. Palasyuk, M. I. Erements, R. J. Cava, S. Naghavi, F. Casper, V. Ksenofontov, G. Wortmann, and C. Felser, *Nat. Mater.* **8**, 630 (2009).
- ¹¹Y. Mizuguchi and Y. Tokano, *J. Phys. Soc. Jpn.* **79**, 102001 (2010).
- ¹²A. Martinelli, A. Palenzona, M. Tropeano, C. Ferdeghini, M. Putti, M. R. Cimberle, T. D. Nguyen, M. Affronte, and C. Ritter, *Phys. Rev. B* **81**, 094115 (2010).
- ¹³M. D. Lumsden and A. D. Christianson, *J. Phys. Condens. Matter.* **22**, 203203 (2010).
- ¹⁴C. C. Lee, W. G. Yin, and W. Ku, *Phys. Rev. Lett.* **103**, 267001 (2009).
- ¹⁵F. Krüger, S. Kumar, J. Zaanen, and J. van den Brink, *Phys. Rev. B* **79**, 054504 (2009).
- ¹⁶W. Schuster, H. Mkiler, and K. Komarek, *Monat. für Chem.* **110**, 1153 (1979).
- ¹⁷M. H. Fang, H. M. Pham, B. Qian, T. J. Liu, E. K. Vehstedt, Y. Liu, L. Spinu, and Z. Q. Mao, *Phys. Rev. B* **78**, 224503 (2008).
- ¹⁸K. W. Yeh, T. W. Huang, Y. L. Huang, T. K. Chen, F. C. Hsu, P. M. Wu, Y. C. Lee, Y. Y. Chu, C. L. Chen, J. Y. Luo, D. C. Yan, and M. K. Wu, *Europhys. Lett.* **84**, 37002 (2008).
- ¹⁹W. Bao, Y. Qiu, Q. Huang, M. A. Green, P. Zajdel, M. R. Fitzsimmons, M. Zhernenkov, S. Chang, M. Fang, B. Qian, E. K. Vehstedt, J. Yang, H. M. Pham, L. Spinu, and Z. Q. Mao, *Phys. Rev. Lett.* **102**, 247001 (2009).
- ²⁰S. Li, C. de la Cruz, Q. Huang, Y. Chen, J. W. Lynn, J. Hu, Y. L. Huang, F. C. Hsu, K. W. Yeh, M. K. Wu, and P. Dai, *Phys. Rev. B* **79**, 054503 (2009).
- ²¹[<http://elk.sourceforge.net>]
- ²²J. P. Perdew and Yue Wang, *Phys. Rev. B* **45**, 13244 (1992).
- ²³J. P. Perdew, A. Ruzsinszky, G. I. Csonka, O. A. Vydrov, G. E. Scuseria, L. A. Constantin, X. Zhou, and K. Burke, *Phys. Rev. Lett.* **100**, 136406 (2008).
- ²⁴T. L. Xia, D. Hou, S. C. Zhao, A. M. Zhang, G. F. Chen, J. L. Luo, N. L. Wang, J. H. Wei, Z. Y. Lu, and Q. M. Zhang, *Phys. Rev. B* **79**, 140510 (2009).
- ²⁵P. Kumar, A. Kumar, S. Saha, D. Muthu, J. Prakash, S. Patnaik, U. Waghmare, A. Ganguli, and A. Sood, *Solid State Commun.* **150**, 557 (2010).
- ²⁶K. Okazaki, S. Sugai, S. Niitaka, and H. Takagi, e-print [arXiv:1010.2374](https://arxiv.org/abs/1010.2374).
- ²⁷T. Yildirim, *Physica C* **469**, 425 (2009).
- ²⁸M. J. Han and S. Y. Savrasov, *Phys. Rev. Lett.* **103**, 067001 (2009).
- ²⁹W. Baltensperger and J. S. Helman, *Helv. Phys. Acta* **41**, 668 (1968); W. Baltensperger, *J. Appl. Phys.* **41**, 1052 (1970).
- ³⁰D. J. Lockwood and M. G. Cottam, in *Magnetic Excitations and Fluctuations II*, edited by U. Balucani, S. W. Lovesey, M. G. Rasetti, and V. Tognetti (Springer, Berlin, 1987), p. 186.
- ³¹D. J. Lockwood and M. G. Cottam, *J. Appl. Phys.* **64**, 5876 (1988).
- ³²C. Y. Moon and H. J. Choi, *Phys. Rev. Lett.* **104**, 057003 (2010).
- ³³K. Horigane, H. Hiraka, and K. Ohoyama, *J. Phys. Soc. Jpn.* **78**, 074718 (2009).
- ³⁴P. G. Radaelli and S. W. Cheong, *Phys. Rev. B* **66**, 094408 (2002).
- ³⁵E. S. Zhitlukhina, K. V. Lamonova, S. O. Orel, P. Lemmens, and Yu. G. Pashkevich, *J. Phys. Condens. Matter* **119**, 156216 (2007).
- ³⁶O. V. Gornostaeva, V. M. Shatalov, and Yu. G. Pashkevich, *JETP Letters* **89**, 167 (2009).
- ³⁷S. H. Lee, G. Xu, W. Ku, J. S. Wen, C. C. Lee, N. Katayama, Z. J. Xu, S. Ji, Z. W. Lin, G. D. Gu, H. B. Yang, P. D. Johnson, Z. H. Pan, T. Valla, M. Fujita, T. J. Sato, S. Chang, K. Yamada, and J. M. Tranquada, *Phys. Rev. B* **81**, 220502 (2010).
- ³⁸M. Granath, J. Bielecki, J. Holmlund, and L. Börjesson, *Phys. Rev. B* **79**, 235103 (2009).
- ³⁹K.-Y. Choi, D. Wulferding, P. Lemmens, N. Ni, S. L. Bud'ko, and P. C. Canfield, *Phys. Rev. B* **78**, 212503 (2008); K.-Y. Choi, P. Lemmens, I. Eremin, G. Zwicknagl, H. Berger, G. L. Sun, D. L. Sun, and C. T. Lin, *J. Phys. Condens. Matter* **22**, 115802 (2010).
- ⁴⁰M. Rahlenbeck, G. L. Sun, D. L. Sun, C. T. Lin, B. Keimer, and C. Ulrich, *Phys. Rev. B* **80**, 064509 (2009).
- ⁴¹L. Chauvière, Y. Gallais, M. Cazayous, A. Sacuto, M. A. Méasson, D. Colson, and A. Forget, *Phys. Rev. B* **80**, 094504 (2009).